AIAA JOURNAL
Vol. 42, No. 6, June 2004

Force-Limited Vibration Complex Two-Degree-of-Freedom System Method

Andre Cote*
EMS Technologies, St-Anne-de-Bellevue, Québec H9X 3R2, Canada
Ramin Sedaghati†
Concordia University, Montréal, Québec H3G 1M8, Canada
and
Yvan Soucy‡
Canadian Space Agency, Saint-Hubert, Québec J3Y 8Y9, Canada

Force-limited vibration testing developed at the Jet Propulsion Laboratory offers many opportunities to decrease the overtesting problem associated with traditional vibration testing. Among the force-limited vibration methods, the complex two-degree-of-freedom system (TDOFS) appears to be the most complete and versatile model that gives reasonably conservative force limits and does not require extrapolation of interface force data for similar mounting structures and test articles. However, there are some limitations to the complex TDOFS model. The model is well adapted for nicely separated modes, but issues regarding the closely space modes have not been fully addressed in the literature. Also, the complex TDOFS model is based on free boundary conditions for the mounting structure, which appear to be natural for many cases such as spacecraft mounted on a launch vehicle. However, this is not necessarily true for some other cases such as an electronic component mounted on a spacecraft antenna, which requires fixed boundary conditions. Greater insights into the complex TDOFS method are given, and methodologies to overcome its limitations are proposed. It is shown that a simple approach can be used to assure conservative estimate of the force limits in situations regarding closely spaced modes. It is also demonstrated that, although the complex TDOFS method is not perfectly adapted to fixed boundary conditions of the mounting structure, given certain precautions, it still provides good estimates of the force limits.

I. Introduction

In conventional vibration testing of space hardware, the acceleration input at the base of the test unit is controlled to specifications, namely, the envelope of the acceleration peaks of the flight environment. This conventional approach to testing is known to overtest greatly the test article at its own resonance frequencies. The penalty of overtesting appears in design and performance compromises, as well as in high costs and schedule overruns associated with recovery from artificial test failures, which would have not occurred during the flight.

An improved vibration test approach was developed and implemented at NASA Jet Propulsion Laboratory (JPL), in the 1990s.[1] The approach is called force-limited vibration (FLV) testing. In addition to controlling the input acceleration, the FLV testing measures and limits the reaction forces between the test article and the shaker through real-time notching of the input acceleration. Thus far FLV testing verification has been done through comparison with data from higher-level acoustic or random vibration tests,[1,2] and with a limited amount of flight data.[3]

Several methods have been developed to estimate the force limits. An example is the blocked-force method,[4] which requires impedance information on only the mounting structure. However, according to Scharton[1] and Kaufman,[5] the blocked-force method is very conservative for most aerospace structures. Also, it does not use the readily available impedance information of the test article. JPL's FLV proposed three methods[1]: the semi-empirical method, the simple two-degree-of-freedom system (TDOFS) method, and the complex TDOFS method. The semi-empirical method derives the force limits without requiring specific information on the mounting structures.[1,6,7] However, they are based on the extrapolation of interface force data for similar mounting structures and test articles and/or comparison with the TDOFS methods and other parameters.[8] The simple TDOFS method uses a simple a spring–mass–damper model to predict the force limits. It also requires information on the mounting structure. This simple method generally gives reasonably conservative force limits. However, the model is sometimes deficient because it neglects the contribution of modes with natural frequencies away from the exciting frequency (residual mass effect).[1] This led to the development of the complex TDOFS method, which uses a slightly more complex spring–mass–damper model to predict the force limits. The complex TDOFS model appears to be the most complete and versatile model. It does require information on the mounting structures. However, some questions remain on the complex TDOFS model. The model is well adapted for nicely separated modes. However, it is not clear how closely spaced modes should be handled. Also, the complex TDOFS model assumes free boundary conditions for the mounting structure. Although these boundary conditions appear to be natural for a spacecraft mounted on a launch vehicle, this is not necessarily true for other cases. For example, in the case of an electronic component mounted on a spacecraft antenna, fixed boundary conditions are usually assumed. The main contribution of this paper is to present two new approaches that complement the complex TDOFS method so that it can handle both of these situations. This paper will also provide greater insights into the approximation made by the complex TDOFS on modes with natural frequencies away from the excitation frequency.

The paper starts with a review of the complex TDOFS method. A discussion follows on the contribution of the modes with natural frequencies away from the exciting frequency and on approaches to

Received 11 April 2003; revision received 18 January 2004; accepted for publication 11 February 2004.

*Structural Engineer, Space Structure Department; currently Vibration Specialist Engineer, Structure and Bogies Group, Bombardier Transportation, St-Bruno, Québec J3V 6E6, Canada; andre.cote@ca.transport.bombardier.com.

†Assistant Professor, Department of Mechanical and Industrial Engineering; sedagha@alcor.concordia.ca. Member AIAA.

‡Structural Dynamics Engineer, Space Technologies; Yvan.Soucy@space.gc.ca.

estimate it. This clears the way for the presentation of the closely spaced mode investigation. It is shown that a simple approach can be used to assure a conservative estimate of the force limits. Then, it is demonstrated that, although the complex TDOFS method is not perfectly adapted to fixed boundary conditions, given certain precautions, it still gives good estimates of the force limits. Finally, a short example is given using an electronic component mounted on a typical spacecraft panel.

II. FLV Method: Complex TDOFS

A. General Approach

In FLV TDOFS jargon, the unit that needs to be tested is called the load, and the unit where the load sits during launch is called the source. Figure 1 presents the general approach proposed by FLV complex TDOFS to determine the interface force specification.

The frequency spectrum is first divided into frequency bands (usually one-third octave bands). Then, the first (or next) frequency band is selected. With reference to Fig. 1, steps 3–7 are performed for the frequency band selected. In steps 3 and 4, simple models are developed to estimate the relation between the interface acceleration and force for each component independently (load and source). In the fifth step, both models are simply coupled together. With use of this newly coupled model, step 6 is to perform a sensitivity study to determine the worst-case ratio of the interface force to the interface acceleration. In this study, the natural frequencies of the load, and of the source are varied within a certain range, and the worst-case scenario is extracted. In step 7, this ratio is multiplied by the acceleration specification of the load to obtain the force specification. Finally, this process is repeated until all frequency bands are covered.

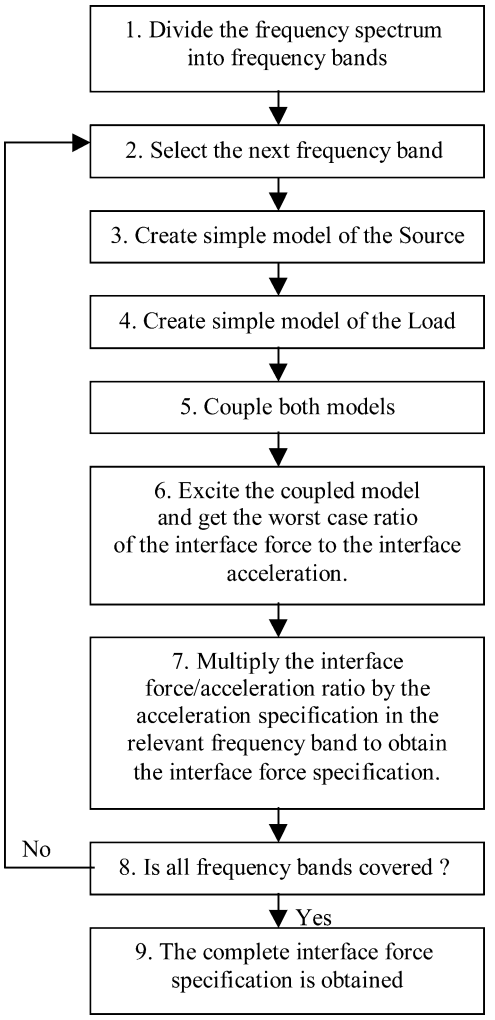

Fig. 1 Outline of the FLV complex TDOFS approach to obtain the interface force specification.

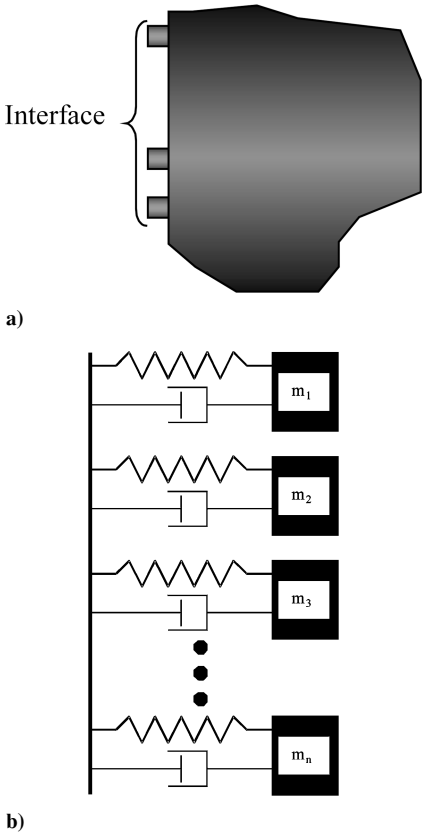

Fig. 2 Asparagus patch model: a) structure with three tiedowns at the interface and b) asparagus model of the structure.

The next section presents a detailed description of the simple model (steps 3 and 4) used to represent the load and the source independently. Section II.C will show how both models are coupled (step 5).

B. Complex TDOFS: Simple Model

The goal of the simple model is to capture the interface behavior of a component. There is no need to obtain the specific information such as the acceleration or stress at some local point; only the interface force and acceleration are sought.

For a structure attached at its base, it can be demonstrated that the relation between the interface force and the interface acceleration is described with the asparagus model shown in Fig. 2 and expressed mathematically as

$$F = \sum_{i=1}^{\infty} m_i H\left(\frac{\omega_i}{\omega}\right)\ddot{U}$$

$$H\left(\frac{\omega_i}{\omega}\right) = \frac{(\omega_i/\omega)^2 + 2j\xi_i(\omega_i/\omega)}{(\omega_i/\omega)^2 - 1 + 2j\xi_i(\omega_i/\omega)} \tag{1}$$

where F is the total base force, $\ddot{U}$ is the base acceleration, m_i is the effective mass of mode i, H is a transfer function, ω is the angular frequency, ω_i is the angular natural frequency of mode i, j is the complex number, and ξ_i is the damping ratio of mode i. The effective mass indicates the sensitivity of each mode to a base excitation (or spatial coupling between each mode and the excitation).[9,10] The frequency function H describes the sensitivity of each mode to the excitation frequency (or frequency coupling between the mode and the excitation).

Obviously, each term of the summation of Eq. (1) is also the governing equation of a single spring–damper–mass system. This is the concept expressed by the asparagus patch model, where each mass corresponds to the effective mass of a mode of the structure and where the stiffness of the spring and the damping level of the damper are such that the frequency function H of each mode is respected.

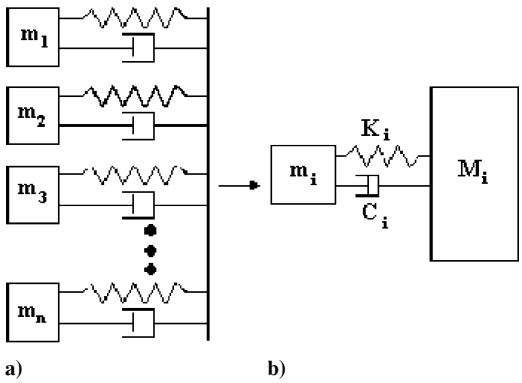

Fig. 3 Simple model of the complex TDOFS: a) complete asparagus patch model and b) simplified asparagus patch model.

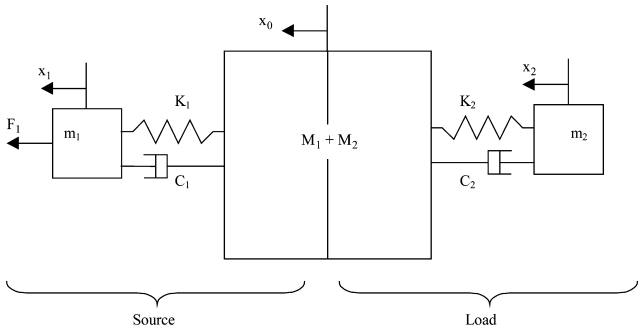

Fig. 4 Coupled model of the complex TDOFS.

The asparagus patch model is then simplified over one frequency band. For a specific frequency band, some modes have natural frequencies lower than the frequency band, some modes have natural frequencies in the frequency band, and some modes have natural frequencies greater than the frequency band. If the excitation frequency is in the frequency band, the asparagus patch model can be simplified to the one presented in Fig. 3. In the simplified model, the modes with natural frequencies lower than the frequency band are ignored. Indeed, for those modes, the frequency function H tends to zero [Eq. (1)]. The modes with natural frequencies higher than the frequency band are considered as a lumped mass. For them, the transfer function tends to unity [Eq. (1)]. The sum of the effective masses of these modes gives the residual mass M_i. Note that this mass is directly attached to the base. The modes with natural frequency in the frequency band must be considered as flexible mode. In the complex TDOFS model, it is assumed that only one mode has a natural frequency in the frequency band. Obviously this is not always the case. In Sec. IV, the effect of considering only one mode when there are actually several is studied.

The simplified asparagus patch model is the model that is used by the complex TDOFS to describe the behavior of the load and of the source. To define the simple model for one specific structure over one specific frequency band, one needs to know the modal behavior of the structure, which is the natural frequencies, the effective masses, and the modal damping. These values could be extracted from a finite element method (FEM) model, experiment, or from experience.

C. Complex TDOFS: Coupled Model

After the creation of a simple model for the load and for the source, the next step is to couple them at their interface. Figure 4 presents the coupled model, which is composed of three masses: the effective mass of the source, the effective mass of the load, and the residual masses of the load and source attached together. The interface is at the attachment of the residual masses.

Note that the coupled model has free boundary conditions.[1] The case where the source is attached to rigid points has not been studied by JPL. The fixed-base boundary condition for the source is addressed in Sec. V.

It is with this model that the complex TDOFS method performs a sensitivity study on the natural frequencies of the effective masses to extract the worst (largest) ratio of the interface force to the interface acceleration (Fig. 1). In this sensitivity survey, the coupled system is excited by a force acting directly on the effective mass of the source. It is thought that this is the most typical case as well as the one that yields the greatest force limits when the masses of the source and of the load are similar.[1]

III. Critically Damped Apparent Mass as Residual Mass

In Sec. II.B, the asparagus model was reduced to a two-DOF model. In this way, modes with natural frequencies outside the frequency band of interest were approximated. Hence, the concept of residual mass was introduced. Scharton[1] described another approach to approximate the contribution of the modes outside the frequency band of interest, which is called critically damped apparent mass. This latter approximation is especially useful during an experiment because it is significantly easier to estimate from measured response than the residual mass. However, what is the extent of these approximations and which method is the best are not clear.

This section provides greater insights into the approximation made by the complex TDOFS on modes with natural frequencies away from the excitation frequency. In this section, first, the residual mass and the critically damped apparent mass approaches are discussed and compared, and then, the extent of the approximations made by these approaches is addressed.

A. Residual Mass Approach

Let us rewrite Eq. (1) to describe the asparagus patch model in a more detailed representation:

$$\frac{F}{\ddot{U}} = \overbrace{\sum_{i=1}^{\nu-1} m_i H\left(\frac{\omega_i}{\omega}\right)}^{\text{Lower modes}} + \overbrace{m_\nu H\left(\frac{\omega_\nu}{\omega}\right)}^{\text{Flexible mode}} + \overbrace{\sum_{i=\nu+1}^{\infty} m_i H\left(\frac{\omega_i}{\omega}\right)}^{\text{Higher modes}} \quad (2)$$

where

$$H\left(\frac{\omega_i}{\omega}\right) = \frac{(\omega_i/\omega)^2 + 2j\xi_i(\omega_i/\omega)}{(\omega_i/\omega)^2 - 1 + 2j\xi_i(\omega_i/\omega)}$$

where F is the interface force, $\ddot{U}$ is the interface acceleration, m_i is the effective mass of mode i, H is a transfer frequency function, ω is the circular frequency, ω_i is the circular natural frequency of mode i, j is the complex number, and ξ_i is the damping ratio. Please note the ratio of the interface force to the interface acceleration is also known as the frequency response function apparent mass.

For lower modes, (ω_i/ω) tends to zero because the excitation frequency is higher than the natural frequencies of the modes. This means that function H tends to zero and so does the contribution of the lower modes to the interface force as shown in Fig. 5. For higher modes, (ω_i/ω) tends to infinity and the function H goes to one. Therefore, the higher modes tend to behave like lumped masses. For a mode with a natural frequency near the excitation frequency $(\omega_i/\omega \approx 1)$, the contribution depends on the amplification factor $Q = 1/(2\xi)$ as the function H tends to $1 - jQ$ (or a modulus very close to Q).

The complex TDOFS method used the trends of the transfer function to derive an approximation. It assumes that the lower modes do not contribute and that the higher modes behave like lumped masses. Figure 6 shows a comparison of this approximation with the transfer function H. The approximation is very good for low- and high-frequency ratio (ω_i/ω). However, as the frequency ratio tends to unity, the approximation becomes less accurate. That is why when a mode has its natural frequency in the frequency band of interest, no approximation is made and the mode is fully considered.

The question of the frequency bandwidth naturally arises. The complex TDOFS method assumes that every mode in the same one-third-octave band as the excitation frequency, which corresponds to frequency ratio of 0.9–1.1, is a flexible mode. From Fig. 6, one could

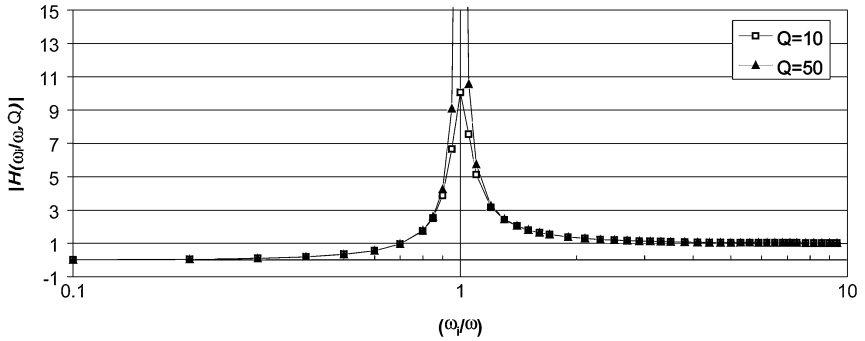

Fig. 5 Frequency function *H* vs frequency.

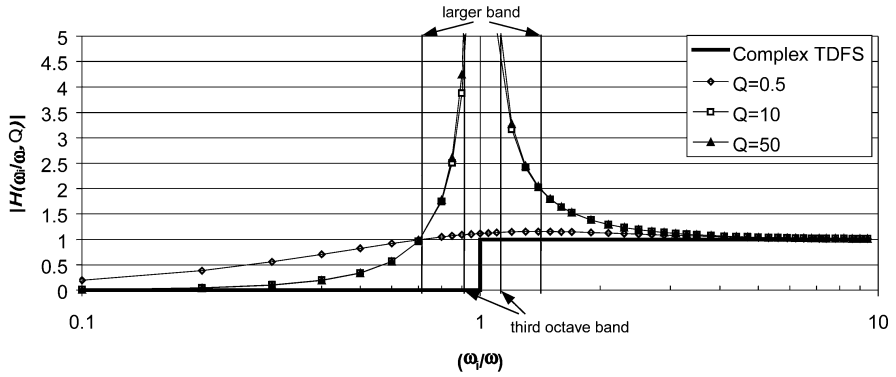

Fig. 6 Frequency function *H* vs frequency with complex TDOFS approximation.

argue that a larger band would be more appropriate. However, such larger bands are likely to include more flexible modes than one-third-octave band.

B. Critically Damped Apparent Mass Approximation

The other approach to estimate the contribution of lower and higher modes is to use the apparent mass with critical damping. Critical damping is obtained when the damping ratio is equal to unity. Figure 6 presents the apparent mass with critical damping ($\xi = 1$ or $Q = 0.5$). First, the critically damped apparent mass shows similar general behavior to the residual mass approximation: For lower modes, it tends to zero, and for higher modes it tends to one. Second, the quality of the approximation is also very close. For higher modes, the performance is about the same. For lower modes, the critically damped apparent mass is more accurate from $\omega_i/\omega = 0.9$ to 0.5 than the residual mass concept. For even lower modes, it is the opposite.

C. Conclusion on the Approximation Approaches

Both methods have shown somewhat similar performance. Therefore, both methods could be used with equal confidence. One advantage that the critically damped apparent mass has over the residual mass concept is during the experiment. Indeed, the critically damped apparent mass can be approximated from a measured apparent mass. Section V will show that the critically damped apparent mass also has another advantage over the residual mass approach, that is, dealing with fixed boundary conditions.

IV. Investigation of Closely Spaced Modes

In the development of the complex TDOFS, it has been assumed that only one mode has its natural frequency in the frequency band of interest. All other modes must have their natural frequencies outside the frequency band of interest. The question of the validity of this approach when more than one mode is present in the frequency band naturally arises.

One approach to consider several modes would be to develop a model similar to the simplified asparagus patch model but with several dynamic masses. (Note that, in this paper, the term dynamic mass is used as to represent a mass supported by the spring and damper and a lumped mass is a mass directly attached to the base.) This would, however, complicate things a lot in terms of theoretical development. Another approach is to use a single effective mass, but where the value of the mass is the sum of the effective mass of the modes present in the frequency band of interest. It is shown that the sum of the effective masses represents a conservative approach.

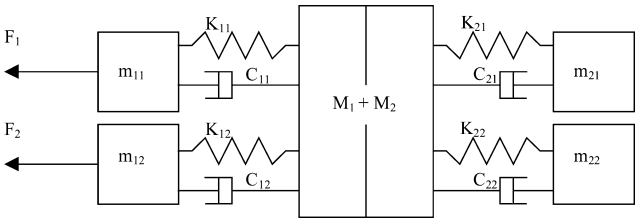

Fig. 7 Complex 3DOFS.

To show that the complex TDOFS with the sum of effective masses method is conservative, the following approach is used. First, the worst-case ratios of the complex TDOFS are obtained for a large set of effective and residual masses covering almost all practical situations: $m_1/M_1 = 8, 4, 2, 1, 0.5, 0.25, 0.125$, and 0; $m_2/M_2 = 8, 4, 2, 1, 0.5, 0.25, 0.125$, and 0; and $M_2/M_1 = 0.001, 0.003, 0.01, 0.03, 0.1, 0.3, 1, 3$, and 10. Please note that these are the same values as studied by Scharton.[1]

Second, the same exercise is performed with a new three-degrees-of-freedom system complex 3DOFS. Figure 7 presents the schematic view of the 3DOFS. Two 3DOFSs are coupled together to consider a coupled load plus source. It is very similar to the complex TDOFS model as shown in Fig. 4 except that two dynamic masses are considered for each system. The coupled system also has free boundary conditions.

However, because the complex 3DOFS has two dynamic masses instead of one per component, additional steps are performed. For each configuration of effective and residual masses, $m_1/M_1, m_2/M_2$,

and M_2/M_1, the effective masses of the complex 3DOFS are varied as follows.

First, $m_{11}+m_{12}=m_1$ and $m_{21}+m_{22}=m_2$; this simply assures, without loss of generality, that the results of the complex 3DOFS are comparable to the results of the complex TDOFS with summed effective masses.

Second, m_{11}/m_{12} and m_{21}/m_{22} go from 10% up to 90% by increments of 10%; this assures that large variety of effective masses are considered for the complex 3DOFS.

With this approach, a sensitivity study on the natural frequencies of the effective masses is performed to extract the maximum ratio as predicted by the complex 3DOFS model for every configuration of effective and residual masses. Note that a precaution was made to ensure that the effective mass of the complex TDOFS is equal to the sum of the effective masses of the complex 3DOFS ($m_{11}+m_{12}=m_1$ and $m_{21}+m_{22}=m_2$) to compare both methods and specify which one gives the greatest ratios.

Table 1 shows the difference in percentage between the results from the complex 3DOFS and the complex TDOFS with summed effective masses. It is clear that the worst cases for the complex 3DOFS are similar (up to a certain accuracy) to the complex TDOFS with summed effective masses, which confirms that the complex TDOFS with summed effective masses is more conservative. For most of the cases, the difference is null. For some cases, the difference is about 5%. Investigations have shown that these differences come from the accuracy used during the frequency sensitivity survey performed to extract the worst-case ratios (Fig. 1), which should be neglected.

To summarize, the complex TDOFS with summed effective mass is in good agreement with the complex 3DOFS and it is also more conservative. Thus, it can be concluded that when several modes are present in the frequency band of interest, the complex TDOFS approach can be used conservatively if the precaution has been taken so that the effective mass of the model represents the sum of the effective masses of every mode in the frequency band.

V. Fixed Base Boundary Condition for the Source

The complex TDOFS method has been developed for a system with free boundary conditions.[1] This kind of system is natural for the case of a spacecraft (load) with a launch vehicle (source). However, for other cases such as an antenna (load) with a spacecraft (source), it seems more natural to have a system with a fixed boundary condition (at the source). A schematic of the coupled model with fixed base boundary condition for the source is shown in Fig. 8.

In the development of the complex TDOFS, a model to represent the apparent mass of the free source was developed. This section investigates the performance of the complex TDOFS for a fixed source.

A. Apparent Mass of a Fixed System

It can be shown (Appendix), that the apparent mass for a fixed system is given by

$$\frac{F}{\ddot{U}} = \sum_{i=1}^{n} \bar{m}_i \bar{H}\left(\frac{\omega_i}{\omega}\right) \tag{3}$$

where

$$\bar{H}\left(\frac{\omega_i}{\omega}\right) = \frac{(\omega_i/\omega)^2 \times (\omega_i/\omega)^2}{(\omega_i/\omega)^2 - 1 + 2j\xi_i(\omega_i/\omega)}$$

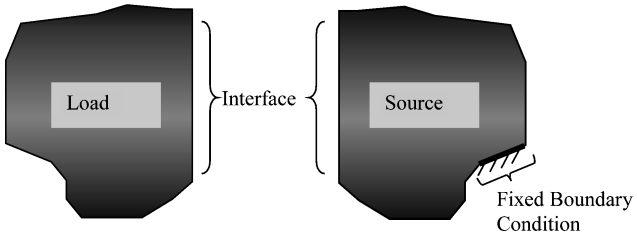

Fig. 8 Coupled model with fixed base source.

Table 1 Difference in percentage between the complex 3DOFS and the complex TDOFS (with the sum of effective mass approximation)

		M_2/M_1								
m_1/M_1	m_2/M_2	0.001	0.003	0.01	0.03	0.1	0.3	1	3	10
8	8	0	0	0	0	0	0	0	0	0
8	4	0	0	0	0	0	0	0	0	0
8	2	0	0	0	0	0	0	0	0	0
8	1	0	0	0	0	0	0	0	0	0
8	0.5	0	0	0	0	0	0	0	0	0
8	0.25	0	0	0	0	0	0	0	0	0
8	0.125	0	0	0	0	0	0	0	0	0
8	0	−5	−5	−5	−5	−5	−5	−5	−5	−5
4	8	0	0	0	0	0	0	0	0	0
4	4	0	0	0	0	0	0	0	0	0
4	2	0	0	0	0	0	0	0	0	0
4	1	0	0	0	0	0	0	0	0	0
4	0.5	0	0	0	0	0	0	0	0	0
4	0.25	0	0	−1	0	0	0	0	0	0
4	0.125	0	0	−1	0	0	0	0	0	0
4	0	−5	−5	−5	−5	−5	−5	−5	−5	−5
2	8	0	0	0	0	0	0	0	1	0
2	4	0	0	0	0	0	0	0	0	0
2	2	0	0	0	0	0	0	0	0	0
2	1	−1	−1	0	0	0	0	0	0	0
2	0.5	0	−1	0	0	0	0	0	0	0
2	0.25	0	0	0	0	0	0	0	1	0
2	0.125	0	1	0	−1	0	0	0	0	0
2	0	−5	−5	−5	−5	−5	−5	−5	−5	−5
1	8	−1	0	0	0	0	0	0	0	0
1	4	1	0	0	0	0	0	0	0	0
1	2	0	0	0	0	0	0	0	0	0
1	1	0	1	1	0	0	0	0	0	0
1	0.5	0	1	1	0	0	0	0	1	0
1	0.25	0	0	−1	1	0	0	0	0	0
1	0.125	0	0	0	−1	0	−1	0	0	1
1	0	−5	−5	−5	−5	−5	−5	−5	−5	−5
0.5	8	1	0	0	0	0	0	0	0	0
0.5	4	1	1	1	0	0	0	0	0	0
0.5	2	1	1	0	1	0	0	0	0	0
0.5	1	1	1	0	1	0	0	0	0	0
0.5	0.5	1	1	2	−1	0	0	0	0	0
0.5	0.25	1	1	3	1	1	0	1	0	0
0.5	0.125	1	1	3	1	0	1	0	0	0
0.5	0	−5	−5	−5	−5	−5	−5	−5	−5	−5
0.25	8	0	1	0	0	0	0	0	0	0
0.25	4	3	1	0	0	0	0	0	0	0
0.25	2	1	2	1	0	0	0	0	0	0
0.25	1	−1	1	1	0	1	0	1	0	0
0.25	0.5	−1	−1	−1	2	0	0	1	0	1
0.25	0.25	−1	−1	1	3	1	0	0	1	1
0.25	0.125	0	0	1	−1	0	1	0	0	−1
0.25	0	−5	−5	−5	−5	−5	−5	−5	−5	−5
0.125	8	−1	1	−1	0	0	0	0	0	0
0.125	4	4	2	2	0	1	0	0	0	0
0.125	2	0	1	2	1	0	0	0	0	0
0.125	1	0	0	−1	3	1	1	0	1	0
0.125	0.5	0	0	3	2	2	1	1	1	0
0.125	0.25	0	0	0	1	0	0	0	1	−1
0.125	0.125	0	0	0	1	3	1	1	1	0
0.125	0	−5	−5	−5	−5	−5	−5	−5	−5	−5
0	8	2	3	1	0	0	0	0	0	0
0	4	2	2	2	1	0	0	0	0	0
0	2	1	1	3	2	1	0	0	0	0
0	1	0	1	3	2	2	1	1	0	0
0	0.5	0	0	2	3	2	1	1	1	0
0	0.25	0	0	2	2	2	2	0	0	1
0	0.125	1	1	1	1	1	3	1	1	1
0	0	−5	−5	−5	−5	−5	−5	−5	−5	−5

This equation is similar to Eq. (1). Variable $\bar{m}_i$, called the equivalent effective mass, does not depend on the frequency but does depend on mode i as does variable m_i from Eq. (1). The frequency function $\bar{H}(\omega_i/\omega)$ is slightly different than the frequency function H from Eq. (1), which is rewritten as

$$H\left(\frac{\omega_i}{\omega}\right) = \frac{(\omega_i/\omega)^2 + 2j\xi_i(\omega_i/\omega)}{(\omega_i/\omega)^2 - 1 + 2j\xi_i(\omega_i/\omega)} \tag{4}$$

The difference is in the numerator. Function H has a damping term, whereas function $\bar{H}(\omega_i/\omega)$ does not have any in the numerator. Also, and most important, function $\bar{H}(\omega_i/\omega)$ has the ratio (ω_i/ω) to the power of 4 instead of 2. Figure 9 presents the comparison of the frequency function of a fixed and free source.

For a low (ω_i/ω) ratio, the frequency functions are about the same. Around the natural frequency, the frequency functions are mostly governed by the amplification factor, and again they are similar for both boundary conditions. However, for a high (ω_i/ω) ratio, the frequency functions are quite different. Whereas the frequency function of a free source goes to one, for a fixed source it goes to infinity. Indeed, at low frequencies, a fixed structure behaves like a rigid structure that cannot moved (neglecting static stiffness effect).

B. Approximation of the Fixed Source Apparent Mass

The complex TDOFS model reviewed in Sec. II.B is made of a lumped mass and a spring–mass–damper system:

$$F/\ddot{U} = \underbrace{m_a H(\omega_i/\omega)}_{\text{spring-mass-damper}} + \underbrace{M_b}_{\text{lumped mass}} \tag{5}$$

where $H(\omega_i/\omega)$ is the frequency function given in Eq. (4) and m_a and M_b are real constants. In Sec. II, it was shown that this model gives a good approximation for a free system. To study the performance of the complex TDOFS model for a fixed system, Eq. (3) can be expanded into three terms:

$$F = \overbrace{\sum_{i=1}^{\nu-1} \bar{m}_i \bar{H}\left(\frac{\omega_i}{\omega}\right)\ddot{U}}^{\text{Lower modes}} + \overbrace{\bar{m}_\nu \bar{H}\left(\frac{\omega_\nu}{\omega}\right)\ddot{U}}^{\text{Flexible mode}} + \overbrace{\sum_{i=\nu+1}^{n} \bar{m}_i \bar{H}\left(\frac{\omega_i}{\omega}\right)\ddot{U}}^{\text{Higher modes}} \tag{6}$$

1) The exciting frequency is significantly above the natural frequencies of lower modes. In this case, the frequency function tends to zero. For example, Fig. 9 presents the case where the ratio ω_i/ω equals 0.5, and the frequency spectrum is divided into one-third-octave bands. Over the defined frequency range, the frequency function is then very close to zero. Therefore, these modes can be neglected. Please note that a similar approximation is made for a source with free boundary conditions (Sec. II).

2) The exciting frequency is close to the natural frequency of the flexible mode. Therefore, it must be fully considered. The response of this mode can be approximated with a spring–mass–damper system such as the one defined in Eq. (5). The mass term m_a equals $\bar{m}_\nu$, and $\bar{H}$ can be approximated by H. Indeed, the frequency function $\bar{H}$ is similar to the frequency function H when the excitation frequency is close to the natural frequency (Fig. 9). Basically, in that case, the frequency function is governed by the damping.

3) The exciting frequency is significantly below the natural frequencies of the higher modes. In this case, the frequency function increases with the ratio (ω_i/ω). The best approximation that can be made with a lumped mass is to use the average value over the defined frequency band (Fig. 9, for example), which can be approximated with $\bar{m}_i \bar{H}(\omega_i/\omega_c)$, where ω_c is the angular frequency at the center of the frequency band. Therefore, considering all of the higher modes, the lumped mass term of Eq. (5),

$$M_b = \sum_{i=1}^{\infty} \bar{m}_i \bar{H}\left(\frac{\omega_i}{\omega_c}\right)$$

This approximation seems rather crude. However, one must bear in mind that the force limits are useful around natural frequencies. The excited mode (or flexible mode) then makes the most important contribution to the interface force. The lower and higher modes are a complement to this response.

Therefore, if the equivalent effective mass terms $\bar{m}_i$ are known, the complex TDOFS can be used to approximate the ratio of the interface force to the interface acceleration. In Sec. V.C an approach to estimate the equivalent effective masses is described.

However, here is an example to further express the concept behind the proposed complex TDOFS approximation of the source with fixed boundary condition. Suppose a fixed system with five modes that is to be modeled with the complex TDOFS in the 22.4–28-Hz frequency band. Table 2 presents the characteristics of the system. In Table 2, ω_b is the angular frequency for 22.4 Hz, ω_c is the angular frequency for 25 Hz (center of band), ω_f is the angular frequency for 28 Hz, and finally ω_i is the angular natural frequency. Figure 10 presents the example's fixed source apparent mass. As expected, the apparent mass is very large at low frequencies.

The apparent mass of the system is given by

$$F/\ddot{U} = \bar{m}_1\bar{H}(\omega_1/\omega) + \bar{m}_2\bar{H}(\omega_2/\omega) + \bar{m}_3\bar{H}(\omega_3/\omega) + \bar{m}_4\bar{H}(\omega_4/\omega) + \bar{m}_5\bar{H}(\omega_5/\omega) \tag{7}$$

With use of Fig. 9, Eq. (7) can be approximated with

$$F/\ddot{U} = \bar{m}_1 \times H(\omega_1/\omega) + \bar{m}_2 \times 7 + \bar{m}_3 \times 17 + \bar{m}_4 \times 50 + \bar{m}_5 \times 65 \tag{8}$$

The first mode is in the frequency band; therefore, it is considered as a flexible mode. Furthermore, as shown by Fig. 9, for a mode in the frequency band, function $\bar{H}$ can be replaced by function H. For the second mode, $\bar{H}$ fluctuates over the frequency band. However, using the complex TDOFS, this mode is approximated with a lumped mass. Therefore, only the value at frequency ratio center $(\omega_2/\omega_c = 2.4)$ of function $\bar{H}$ is used. This value is 7.

Table 2 Modal values for fixed source example

Mode	Equivalent effective mass	Natural frequency	ω_i/ω_b	ω_i/ω_c	ω_i/ω_f
1	1.2	25	1.12	1.00	0.89
2	0.7	60	2.68	2.40	2.14
3	0.5	100	4.46	4.00	3.57
4	0.1	175	7.81	7.00	6.25
5	0.1	200	8.93	8.00	7.14

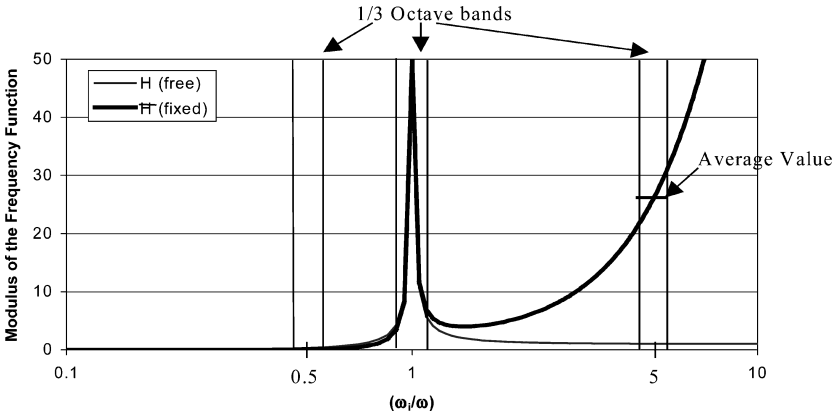

Fig. 9 Comparison of the frequency function between a fixed and free source.

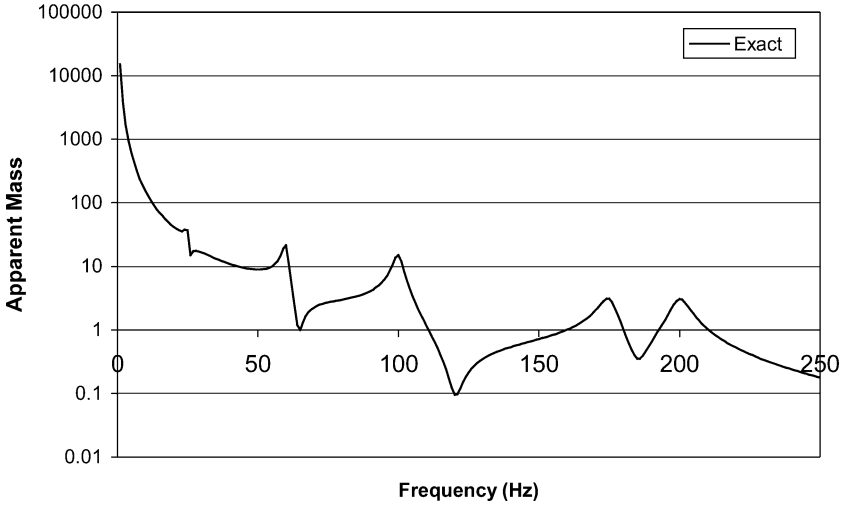

Fig. 10 Apparent mass for fixed source system.

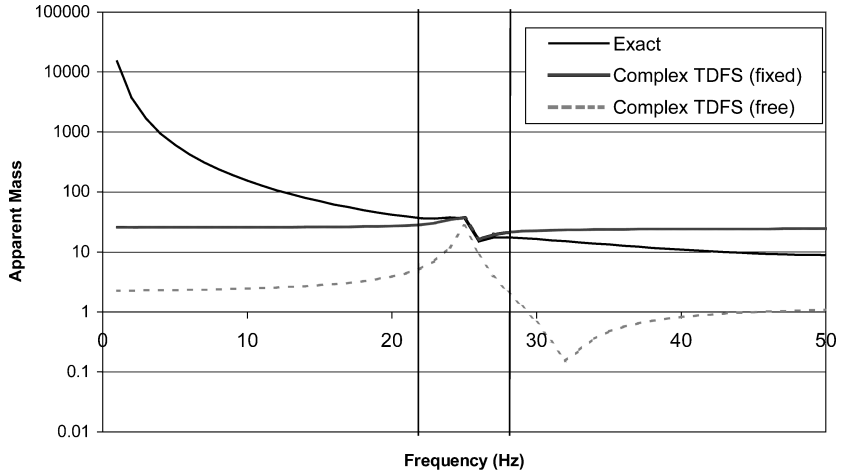

Fig. 11 Apparent mass for fixed source system-approximation of the first mode.

The same approach is used for the third (amplitude = 17), fourth (amplitude = 50), and fifth (amplitude = 65) modes. Then, the contribution of modes 2–5 can be summed, and the complex TDOFS approximation of the system may be described as

$$F/\ddot{U} = \overbrace{1.2 \times H(\omega_2/\omega)}^{\text{Equivalent effective mass term}} + \overbrace{24.9}^{\text{Equivalent residual mass term}} \tag{9}$$

Please note that with the typical free source complex TDOFS, the approximation would be

$$F/\ddot{U} = m_1 \times H(\omega_1/\omega) + m_2 \times 1 + m_3 \times 1 + m_4 \times 1 + m_5 \times 1$$

$$F/\ddot{U} = \overbrace{1.2 \times H(\omega_2/\omega)}^{\text{Effective mass term}} + \overbrace{1.4}^{\text{Residual mass term}} \tag{10}$$

The approximation made by the complex TDOFS with or without special consideration for the fixed boundary condition is presented in Fig. 11. Note that, although the curves are plotted over the whole frequency range, the validity of the approximation by the complex TDOFS is only over the 22.4–28-Hz range. To highlight this, vertical lines in Fig. 11 indicate the valid frequency range.

The comparison between the exact response and the complex TDOFS approximation with special fixed boundary condition consideration is good but not perfect. At the natural frequency, the comparison is very good. However, before the natural frequency, the complex TDOFS slightly underestimate the response, and after the natural frequency, the complex TDOFS slightly overestimates it. As is clear in Fig. 9, the higher mode effect is made of two components: an average amplitude and a fluctuation with frequency. With special consideration, the complex TDOFS can account for the average amplitude but not for the fluctuation with frequency. On average, the complex TDOFS approximation is almost perfect. However, the fluctuation with the frequency is not perfect.

As a reference, the complex TDOFS approximation without any consideration for the fixed boundary condition (called complex TDOFS free) is also presented in Fig. 11. The comparison is not good, even for the average response. Obviously, the fixed boundary condition with special consideration has been a significant improvement to the approximation.

C. Calculation of the Lumped and Equivalent Effective Mass for a Fixed System

In the preceding section, it was shown that the model of Fig. 3 could give a reasonably good approximation of the apparent mass of a fixed system if the dynamic and lumped masses are well defined. This section shows how to determine those values.

In Sec. III, it was shown that the critically damped apparent mass is a good approximation of the lumped mass for a free source. The same approximation may be used for a fixed source. When Eq. (6) rewritten here is used,

$$F(Q) = \overbrace{\sum_{i=1}^{v-1} \bar{m}_i \bar{H}\left(\frac{\omega_i}{\omega}\right)\ddot{U}}^{\text{Lower modes}} + \overbrace{\bar{m}_v \bar{H}\left(\frac{\omega_v}{\omega}\right)\ddot{U}}^{\text{Flexible mode}} + \overbrace{\sum_{i=v+1}^{n} \bar{m}_i \bar{H}\left(\frac{\omega_i}{\omega}\right)\ddot{U}}^{\text{Higher modes}} \tag{11}$$

where

$$\bar{H}\left(\frac{\omega_i}{\omega}\right) = \frac{(\omega_i/\omega)^2 \times (\omega_i/\omega)^2}{(\omega_i/\omega)^2 - 1 + j(1/Q_i)(\omega_i/\omega)}$$

it can be shown that the critically damped, $Q = 0.5$, apparent mass, at the natural frequency of mode v, is

$$\frac{F}{\ddot{U}}(Q=0.5) = \overbrace{\sum_{i=1}^{v-1} \bar{m}_i \bar{H}\left(\frac{\omega_i}{\omega_v}\right)}^{\text{Lower modes}} - \overbrace{0.5 \times j\bar{m}_v}^{\text{Flexible mode}} + \overbrace{\sum_{i=v+1}^{n} \bar{m}_i \bar{H}\left(\frac{\omega_i}{\omega_v}\right)}^{\text{Higher modes}} \tag{12}$$

Because the frequency function only slightly depends on the amplification factor for lower and higher modes as shown in Fig. 12, Eqs. (11) and (12) may be combined to give

$$F/\ddot{U}(Q) \approx \overbrace{F/\ddot{U}(Q=0.5)}^{\text{Lumped mass term}} - \overbrace{j\bar{m}_v(Q-0.5)}^{\text{Equivalent effective mass term}} \tag{13}$$

The amplification factor is generally much larger than 0.5. Thus, Eq. (13) may be simplified to

$$F/\ddot{U}(Q) \approx \overbrace{F/\ddot{U}(Q=0.5)}^{\text{Lumped mass term}} - \overbrace{j\bar{m}_v(Q)}^{\text{Equivalent effective mass term}} \tag{14}$$

The term on the left-hand side is the apparent mass of the system. The first term of the right-hand side is the apparent mass with critical damping. Finally, the second term of the right-hand side is the equivalent effective mass term.

The procedure is then the following. First, get the apparent mass of the source either by the FEM or experimentally. Then, for every mode, the apparent mass and the critically damped apparent mass at the natural frequency should be extracted. Finally, with use of Eq. (14), the equivalent effective mass is obtained for each mode.

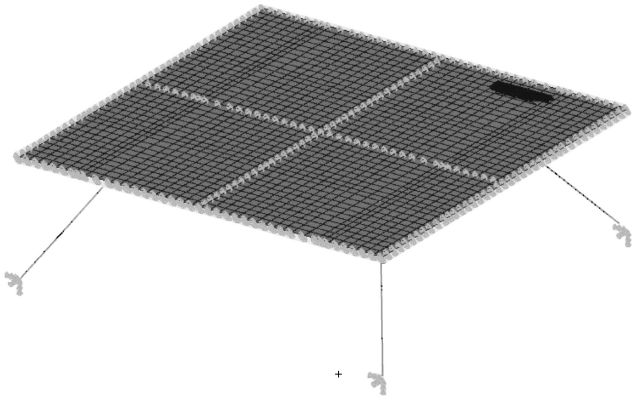

Fig. 15 Boundary conditions of the panel.

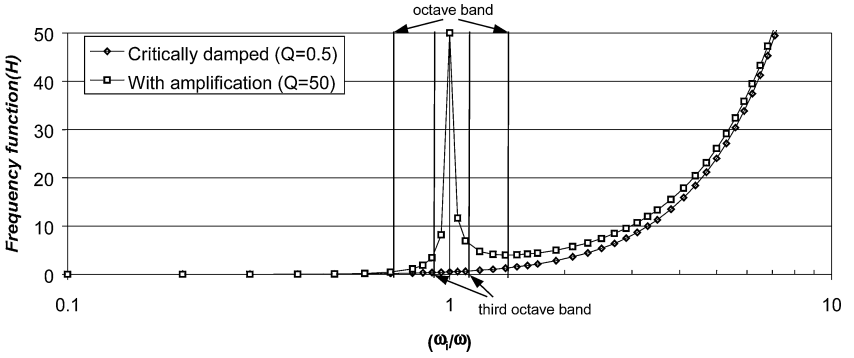

Fig. 12 Comparison of the frequency function for a fixed system with and without amplification.

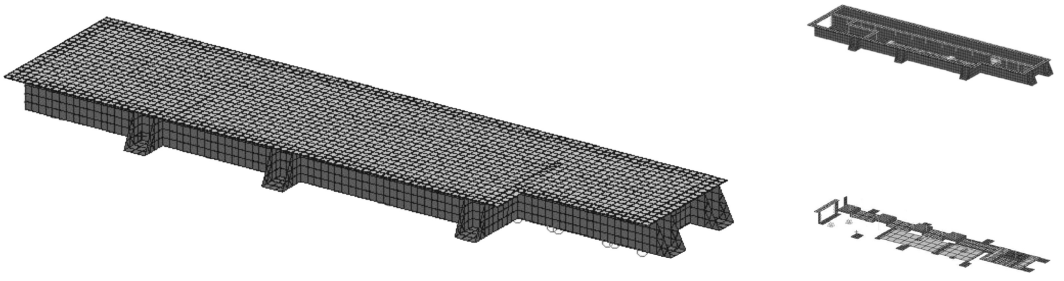

Fig. 13 FEM model of the SSPA.

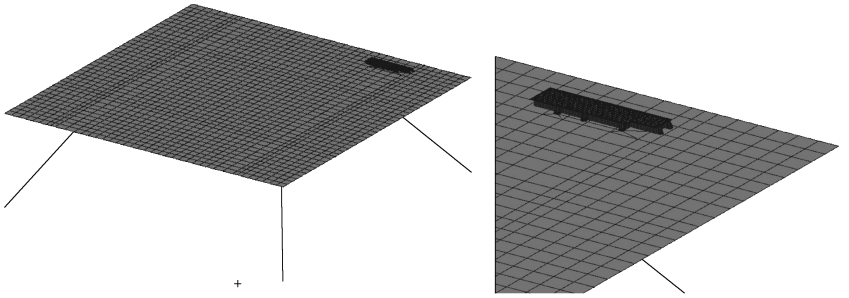

a) Global view **b) Zoom on SSPA location**

Fig. 14 Coupled FEM model of the panel and SSPA.

VI. Practical Implementation on a Typical Flight Unit

To demonstrate the FLV method for a fixed system, a practical example is studied. The solid state power amplifier (SSPA) of an antenna is used as the load, and a typical panel is used as the source. In a first step, the SSPA is presented along with the panel, where it is attached. Then, with use of the FEM models of the SSPA and panel and a typical base acceleration for the panel, the interface force and acceleration expected during launch are calculated. In a third step, the force limit is calculated. Finally, a comparison between the force limits, the expected interface force of the SSPA–panel coupled system (as in launch), and the expected interface force at the base of the SSPA (as in the vibration test of the SSPA) is performed.

A. Presentation of the Flight Units

The units and their finite element models are presented in Figs. 13 and 14. In this system, the load is the SSPA and the source is the panel (including other electronic units that are attached to the same panel). The other electronic units are modeled as nonstructural mass. The SSPA weighs 1.56 lb (0.71 kg) and is roughly 12 in. (0.3048 m) long × 12 in. (0.3048 m) wide.

The panel is supported at its boundary and along the middle lines as shown in Fig. 15 and also with four struts (modeled with CBAR elements).

B. SSPA–Panel System Analysis

Before analyzing the response of the SSPA when subjected to vibration environment (test configuration), the coupled SSPA–panel system is investigated. This system corresponds to the expected response during launch. Therefore, it serves as the reference.

With use of the acceleration input defined in Fig. 16, and the FEM model of the SSPA–panel system, the acceleration and force at the interface between the SSPA and the panel are calculated. The interface acceleration and the interface force are shown in Figs. 17 and 18, respectively. Figure 17 also shows the input acceleration of Fig. 16 and an envelope to the interface acceleration. This envelope corresponds to the input acceleration that is used during the random vibration test of the SSPA.

C. Force Limit Calculation

The force limit is calculated, and Fig. 19 shows the force limits for both simple and complex TDOFS. The average force spectrum[1] has also been shown in Fig. 19.

D. SSPA Analysis

With use of the envelope acceleration defined in Fig. 16 as the input for the random vibration environment, the response of the

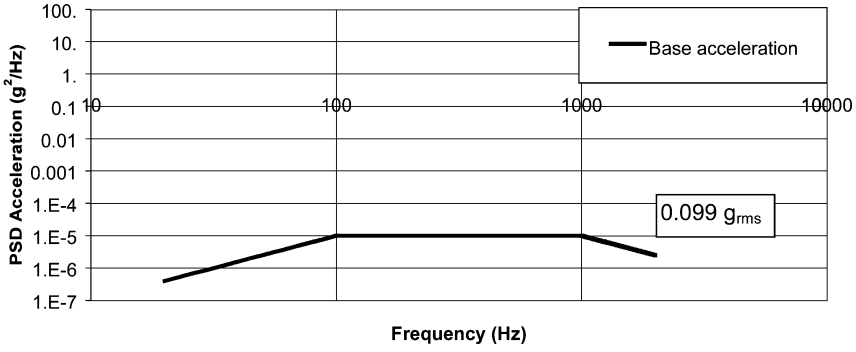

Fig. 16 Input acceleration level at the base of the coupled system.

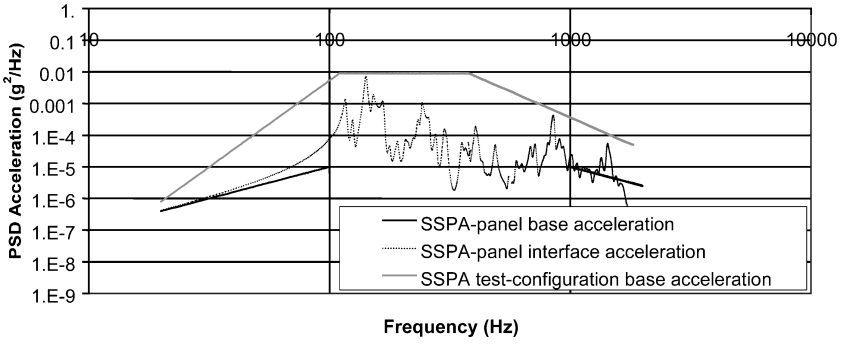

Fig. 17 FEM prediction of the interface acceleration between the SSPA and the support panel.

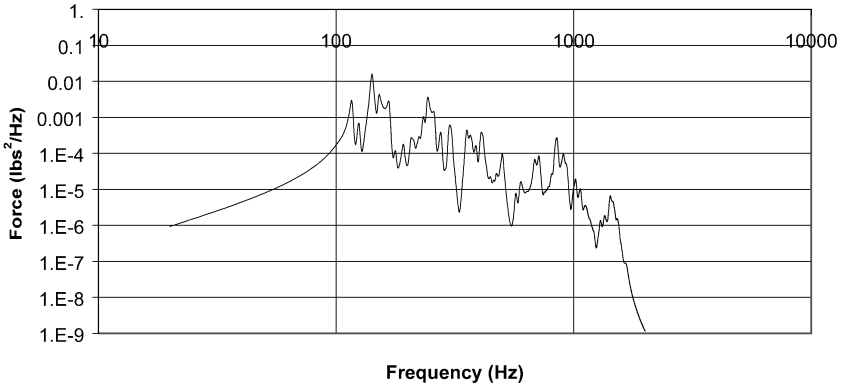

Fig. 18 FEM prediction of the interface force between the SSPA and the support panel.

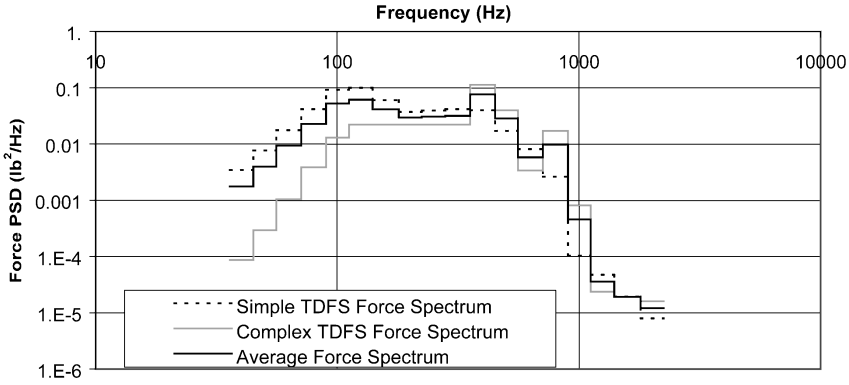

Fig. 19 Force limit for the SSPA test.

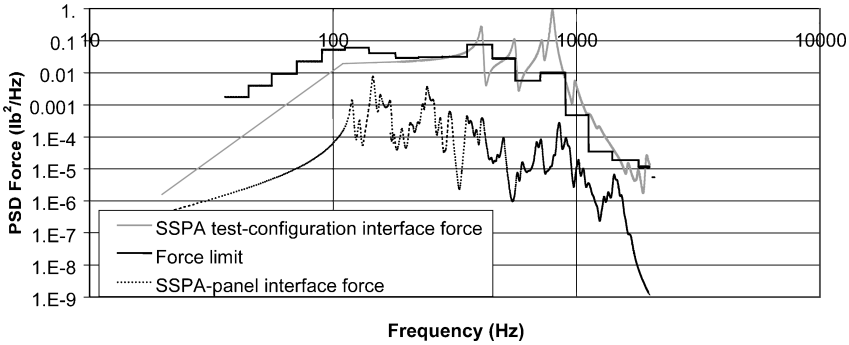

Fig. 20 FEM prediction of the interface force.

SSPA is calculated. Figure 20 shows the interface force response of the SSPA along with the interface force expected in launch and the force limits. It is obvious that the interface force during the vibration test of the SSPA is greater than the expected interface force during launch. It is also seen that the force limits reduces the interface force during the test. The reduction is quite significant because the maximum power spectral density (PSD) peak is reduced by a factor of 90 and the rms value is reduced by a factor of 2.7. However, the interface force still stays greater than the interface force expected during launch; the test is still conservative.

VII. Conclusions

This paper focuses on technical and scientific investigations of the complex TDOFS method of the FLV approach and on practical implementation of the method on a flight unit.

New developments on the FLV approach have been proposed for special cases such as closely space modes, approximation of residual mass with critically damped apparent mass, and fixed boundary condition for the source. It has been shown that if the sum of all modes' effective masses that have their natural frequency inside the frequency band of interest is used (closely spaced modes), the complex TDOFS gives a conservative force limit. On the source fixed boundary condition issues, the investigation has shown that the complex TDOFS method could give a reasonably good approximation of the apparent mass of fixed system if the dynamic and lumped masses are well defined.

Finally, a practical investigation of the FLV method on a typical SSPA has been performed. It has been found that if the vibration test had been undertaken using the FLV approach, the rms interface force would have been reduced by a factor of 2.7 (and a factor of 90 of the peak PSD). Furthermore, interface force during test still would have been quite conservative compared to the interface force during launch. Interestingly, this practical example has been performed with the newly developed consideration for a fixed source.

Appendix: Development of the Apparent Mass for System with Fixed Boundary Condition

The system of equations that govern the source behavior can be expressed as

$$[K]\{x\} + j\omega[C]\{x\} - \omega^2[M]\{x\} = \{F\} \tag{A1}$$

where $[K]$, $[C]$, and $[M]$ are the stiffness, damping, and mass matrices, respectively, $\{x\}$ is the displacement vector, and $\{F\}$ is the exterior force vector.

Because the source is fixed, it is possible to partition for constrained DOF:

$$\left(\begin{bmatrix} K_{ff} & K_{cf} \\ K_{cf} & K_{cc} \end{bmatrix} + j\omega \begin{bmatrix} C_{ff} & C_{cf} \\ C_{cf} & C_{cc} \end{bmatrix} - \omega^2 \begin{bmatrix} M_{ff} & M_{cf} \\ M_{cf} & M_{cc} \end{bmatrix}\right) \begin{Bmatrix} x_f \\ x_c \end{Bmatrix} = \begin{Bmatrix} F_f \\ F_c \end{Bmatrix} \tag{A2}$$

where f indicates free and c constrained. Because $x_c = 0$ by definition, the system of equations can be reorganized as

$$\big([K_{ff}] + j\omega[C_{ff}] - \omega^2[M_{ff}]\big)\{x_f\} = \{F_f\} \tag{A3a}$$

$$\big([K_{cf}] + j\omega[C_{cf}] - \omega^2[M_{cf}]\big)\{x_f\} = \{F_c\} \tag{A3b}$$

where $\{F_c\}$ is the interface force vector at the base of the source and $\{F_f\}$ is the exciting force vector on the source. The required interface forces are the ones between the load and the source. For the rest of this development, it is supposed that the interface between the load and the source is made at only one point (one DOF), and that this DOF is the k one. This is the equivalent to a multipoint interface that moves as a rigid element, which is the hypothesis that is made for the load during testing.

A new partition is made with Eq. (A3a): the interface point (DOF) k and the other DOFs (called s):

$$\left(\begin{bmatrix} K_{ss} & K_{sk} \\ K_{ks} & K_{kk} \end{bmatrix} + j\omega \begin{bmatrix} C_{ss} & C_{sk} \\ C_{ks} & C_{kk} \end{bmatrix} - \omega^2 \begin{bmatrix} M_{ss} & M_{sk} \\ M_{ks} & M_{kk} \end{bmatrix}\right) \begin{Bmatrix} x_s \\ x_k \end{Bmatrix} = \begin{Bmatrix} F_s \\ F_k \end{Bmatrix} \tag{A4}$$

To obtain the impedance at the interface between the load and the source (DOF k), an acceleration is imposed at DOF k. No exterior force is assumed, thus $\{F_s\}$ equals zero. Note that F_k is the

interface force,

$$\big([K_{ss}] + j\omega[C_{ss}] - \omega^2[M_{ss}]\big)\{x_s\}$$

$$= -\big(\{K_{sk}\} + j\omega\{C_{sk}\} - \omega^2\{M_{sk}\}\big)x_k \quad \text{(A5a)}$$

$$\big(\langle K_{ks}\rangle + j\omega\langle C_{ks}\rangle - \omega^2\langle M_{ks}\rangle\big)\{x_s\}$$

$$+ \big(K_{kk} + j\omega C_{kk} - \omega^2 M_{kk}\big)x_k = F_k \quad \text{(A5b)}$$

where { } denotes a column vector and ⟨ ⟩ denotes a row vector. Getting the undamped modal basis out of the free system,

$$\big([K_{ss}]\{x_s\} = \omega^2[M_{ss}]\big)\{x_s\} \Rightarrow \{\phi_i\}, \omega_i \qquad \text{for} \qquad i = 1, s \quad \text{(A6)}$$

where ϕ_i and ω_i^2 are the eigenvector and eigenvalue of mode i, respectively. Projecting Eq. (A5a) on the modal basis and taking the ith row gives

$$\big[\omega_i^2 m_i + j(\omega\omega_i m_i/Q_i) - \omega^2 m_i\big]y_i = -\big\langle\phi_i^t\big\rangle\{A\}x_k$$

where m_i is the modal mass of mode i,

$$\{x_s\} = \sum_{i=1}^{s}\{\phi_i\}y_i, \qquad \{A\} = \big(\{K_{sk}\} + j\omega\{C_{sk}\} - \omega^2\{M_{sk}\}\big) \quad \text{(A7)}$$

Equations (A7) can be rearranged as

$$\{x_s\} = \sum_{i=1}^{s}\{\phi_i\}y_i$$

$$= -\sum_{i=1}^{s}\{\phi_i\}\big\langle\phi_i^t\big\rangle\frac{\{A\}}{\big[\omega_i^2 m_i + j(\omega\omega_i m_i/Q_i) - \omega^2 m_i\big]}x_k \quad \text{(A8)}$$

Inserting Eq. (A8) into Eq. (A5b) gives

$$-\sum_{i=1}^{s}\big(\langle K_{ks}\rangle + j\omega\langle C_{ks}\rangle - \omega^2\langle M_{ks}\rangle\big)\{\phi_i\}\big\langle\phi_i^t\big\rangle$$

$$\times\frac{\{A\}}{\big[\omega_i^2 m_i + j(\omega\omega_i m_i/Q_i) - \omega^2 m_i\big]}x_k$$

$$+ \big(K_{kk} + j\omega C_{kk} - \omega^2 M_{kk}\big)x_k = F_k \quad \text{(A9)}$$

Rearranging once yields

$$-\sum_{i=1}^{s}\frac{\langle A^T\rangle\{\phi_i\}\big\langle\phi_i^t\big\rangle\{A\}}{\big[\omega_i^2 m_i + j(\omega\omega_i m_i/Q_i) - \omega^2 m_i\big]}x_k + Bx_k = F_k \quad \text{(A10)}$$

where

$$\{A\} = \big(\{K_{sk}\} + j\omega\{C_{sk}\} - \omega^2\{M_{sk}\}\big)$$

$$\langle A^T\rangle = \big(\langle K_{ks}\rangle + j\omega\langle C_{ks}\rangle - \omega^2\langle M_{ks}\rangle\big)$$

$$B = \big(K_{kk} + j\omega C_{kk} - \omega^2 M_{kk}\big)$$

and rearranging a second time yields

$$\sum_{i=1}^{s}\frac{\langle A^T\rangle\{\phi_i\}\big\langle\phi_i^t\big\rangle\{A\}\big(1/\omega_i^4\big)\big(\omega_i^4/\omega^4\big)}{m_i\big[(\omega_i/\omega)^2 + j(\omega_i/\omega)(1/Q_i) - 1\big]}\ddot{x}_k - \frac{B\ddot{x}_k}{\omega^2} = F_k \quad \text{(A11)}$$

Finally, with rearrangement a third time, the impedance or apparent mass for a fixed source system is obtained:

$$\frac{F_k}{\ddot{x}_k} = \left[\sum_{i=1}^{s}\bar{m}_i\bar{H}\left(\frac{\omega_i}{\omega}\right)\right] - \frac{B}{\omega^2} \quad \text{(A12)}$$

where

$$\bar{m}_i = \frac{\langle A^T\rangle\{\phi_i\}\big\langle\phi_i^t\big\rangle\{A\}}{m_i\omega_i^4}$$

$$\bar{H}\left(\frac{\omega_i}{\omega}\right) = \frac{\{\omega_i/\omega\}^4}{\big[(\omega_i/\omega)^2 - 1 + j(\omega_i/\omega)(1/Q_i)\big]}$$

The second right-hand-side term of Eq. (A12) is a local effect. Its value is insignificant compared to the first right-hand term. Therefore, it is neglected:

$$\frac{F_k}{\ddot{x}_k} = \sum_{i=1}^{s}\bar{m}_i\bar{H}\left(\frac{\omega_i}{\omega}\right) \quad \text{(A13)}$$

The first term of the summation, $\bar{m}_i$, has the unit of a mass. It is a representation of the contribution of each mode to the apparent mass due to the spatial coupling with the excitation, which is in this case an imposed acceleration. As the counterpart of the free source system, it is called the effective mass of each mode. The second term is the frequency coupling of each mode with the excitation.

Acknowledgments

This paper results from a collaborative effort between the Space Technologies Branch of the Canadian Space Agency, EMS Space and Electronics Group, and Concordia University. The authors acknowledge T. D. Scharton, formerly with the Mechanical Engineering Section of the NASA Jet Propulsion Laboratory, for technical discussions.

References

[1]Scharton, T. D., "Force Limited Vibration Testing Monograph," NASA Reference Publ. RP-1403, May 1997.

[2]Chang, K. Y., and Scharton, T. D., "Verification of Force and Acceleration Specifications for Random Vibration Tests of Cassini Spacecraft Equipment," *Proceedings of the European Conference on Spacecraft Structure*, ESA Publications Div., Noordwijk, The Netherlands, 1996, pp. 911–919.

[3]Scharton, T. D., "In-Flight Measurements of Dynamic Force and Comparison with Methods Used to Derived Force Limits for Ground Vibration Tests," *Proceedings of the European Conference on Spacecraft Structures*, ESA Publications Div., Noordwijk, The Netherlands, 1998, pp. 583–588.

[4]Piersol, A. G., White, P. H., Wilby, J. F., Hipol, P. J., and Wilby, E. G., "Vibration Test Procedures for Orbiter Sidewall-Mounted Payload: Phase 1 Report Appendices," Astron Research and Engineering, Rept. 7114-01, Santa Monica, CA, Nov. 1988.

[5]Kaufman, D. S., "Force Limiting Testing for the Small Explorer Satellite Program at NASA Goddard Space Flight Center," *Journal of the IEST*, Vol. 43, No. 1, 2000, pp. 24–30.

[6]Murfin, W. B., "Dual Specification in Vibration Testing," *Shock and Vibration Bulletin*, No. 38, Pt. 1, 1968, pp. 109–113.

[7]Witte, A. F., and Rodeman, R., "Dual Specification in Random Vibration Testing, an Application of the Mechanical Impedance," *Shock and Vibration Bulletin*, No. 41, Pt. 44, 1970, pp. 109–118.

[8]Soucy, Y., Singhal, R., Lévesque, D., Poirier, R., and Scharton, T. D., "Force Limited Vibration Testing Applied to the FTS Instrument of SCISAT-1," *Proceedings of the ASTRO 2002–12th CASI Conference on Astronautics* [CD-ROM], Canadian Aeronautics and Space Inst., Ottawa, 2002.

[9]Bamford, R. M., Wada, B. K., and Gayman, W. H., "Equivalent Spring-Mass System for Normal Modes," Jet Propulsion Lab., TM 33-3803, California Inst. of Technology, Pasadena, CA, 1971, pp. 1–15.

[10]Sedaghati, R., Soucy, Y., and Etienne, N., "Efficient Estimation of Effective Mass for Complex Structures Under Base Excitations," *Canadian Aeronautics and Space Journal*, Vol. 49, No. 3, 2003, pp. 135–143.

A. Messac
Associate Editor